Metal Coordination to the Formal P=N Bond of an Iminophosphorane and Charge-Density Evidence against Hypervalent Phosphorus(v)[‡]

Nikolaus Kocher, Dirk Leusser, Alexander Murso, and Dietmar Stalke*[a]

Abstract: The iminophosphorane $Ph_2P(CH_2Py)(NSiMe_3)$ (**1**) was treated with deprotonating alkali metal reagents to give $[(Et_2O)Li\{Ph_2P(CHPy)(NSiMe_3)\}]$ (**2**), $[\{Ph_2P(CH_2Py)(NSiMe_3)\}Li\{Ph_2P(CHPy)(NSiMe_3)\}]$ (**3**) and $[\{Ph_2P(CH_2Py)(NSiMe_3)\}Na\{Ph_2P(CHPy)(NSiMe_3)\}]$ (**4**). We report their coordination behaviour in solid-state structures and NMR spectroscopic features in solution. Furthermore, we furnish experimental evidence against hypervalency of the phosphorus atom in iminophosphoranes from experimental charge-density studies and subsequent topological analysis. The topological properties, correlated to the results from NMR spectroscopic investigations, illustrate that the formal P=N double bond is better written as a polar P^+-N^- single bond. Additionally, the effects of metal coordination on the bonding parameters of the iminophosphorane and the related anion are discussed.

Keywords: alkali metals · bond topology · hypervalent compounds · N ligands · P ligands

Introduction

Since the landmark work of Wittig and Geissler[1] and Staudinger and Meyer[2] on phosphonium ylides and iminophosphoranes, respectively, these isoelectronic analogues of phosphane oxides have been well established species in organometallic and organic syntheses.[3] Particularly, the Wittig reaction and its extensions play an outstanding role in the (stereo)selective transformation of ketones and aldehydes into olefins. The P=N bond in polyphosphazenes is known to be thermally very robust and gives access to inert polymeric materials, but the Si–N bond in silylated iminophosphoranes of the general type $R_3P{=}NSiMe_3$ can easily be cleaved in reactions with main group[4] or transition metal halides[5] leading to phosphoraneiminato complexes containing the $[R_3PN]^-$ building block. Recently, Stephan et al. proved the high catalytic activity of these complexes towards ethylene polymerization.[6] Consequently, P=E bonding (E = C, N, O) is an issue of experimental and theoretical debate because of the chemical importance of ylides, iminophosphoranes and phosphane oxides.[7] The P=E bonds in iminophosphoranes are mostly described as a resonance hybrid between a double-bonded ylene $R_3P{=}NR$ and a dipolar ylidic form $R_3P^+-N^-R$.[3,8] Calculations on main group "hypervalent" compounds suggest that although the presence of d-orbitals is necessary to successfully model any of the heavier main group elements, they do not play a significant role in bonding. It has been proposed instead that negative hyperconjunction may be responsible for any π-character in the P–O, P–C or P–N bonds.[7,9] These results have been substantiated by recent calculations dealing with the Wittig-type reactivity of phosphorus ylides[10] and iminophosphoranes[11] and by the experimental determination of the charge density in a phosphane ylide.[12]

Phosphorus-based ligand systems with one or more donating atoms in the periphery are gaining increasing importance in catalysis and in the design of self-assembling ligands.[13] The incorporation of heteroaromatic substituents at the phosphorus centre instead of commonly employed phenyl groups alters and augments the reactivity and coordination capability of the ligand system and leads to the design of multidentate Janus head ligands.[14,15] The concept of side-arm donation, which has already proved to be useful in various catalytic reactions involving chelating phosphanes with selectivity for hard/soft coordination sites,[16] can also be achieved by means of ring heteroatoms (Scheme 1).

Similar to ketones, sulfones and hydrazones,[17] P-alkyl-substituted iminophosphoranes are moderately acidic and can be deprotonated at the C_α-position by lithium organyls. Several alkali metal complexes of α-deprotonated iminophosphoranes have been obtained and structurally characterised. The cations are C,N-chelated by the deprotonated

[a] Dr. N. Kocher, Dr. D. Leusser, A. Murso, Prof. Dr. D. Stalke
Institut für Anorganische Chemie der Universität Würzburg
Am Hubland, 97074 Würzburg (Germany)
Fax: (+49) 931-888-4619
E-mail: dstalke@chemie.uni-wuerzburg.de

[‡] This work was supported by the Deutsche Forschungsgemeinschaft (grant no. Sta 334/8-3 and Graduiertenkolleg 690 *Elektronendichte—Theorie und Experiment*) and Chemetall, Frankfurt/Main.

Supporting information for this article is available on the WWW under http://www.chemeurj.org/ or from the author.

  DOI: 10.1002/chem.200400163

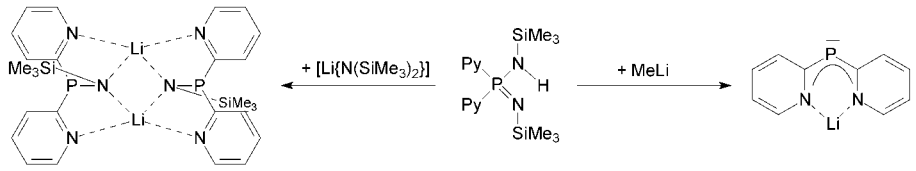

Scheme 1. Reactions implying P=N bond cleavage.

carbon and imino nitrogen atoms. The steric demand of the substituents and the nature of the donor solvents determine the degree of aggregation, which ranges from monomers to tetramers.[8,18] Hence, the introduction of alkyl bridges between the phosphorus atom and the donating heterocycle in the ligand periphery of iminophosphoranes provides not only the opportunity of greater geometrical adaptability due to a wider bite but also to generate anionic species. Delocalisation of the carbanionic charge to the donating atoms would enable the ligand to respond to the various requirements of metals differing in radius and polarisability.

Recently it was shown that *N*-(trimethylsilyl)diisopropyl-2-picolyliminophosphorane $i\mathrm{Pr_2P(CH_2Py)(NSiMe_3)}$ (Py = 2-pyridyl) is a valuable building block in the generation of 1,3-dimetallacyclobutanes $[\mathrm{M\{C(}i\mathrm{Pr_2PNSiMe_3)(Py)\}}]_2$ (M = $\mathrm{Ge^{II}}$, $\mathrm{Sn^{II}}$, $\mathrm{Pb^{II}}$) by single deprotonation with lithium organyls and subsequent reaction with the corresponding Group 14 chloride.[19] Here we report alkali metal complexes derived from *N*-(trimethylsilyl)-diphenyl-2-picolyliminophosphorane (**1**), their coordination behaviour in solid-state structures and their NMR spectroscopic features in solution. Furthermore, we furnish experimental evidence against hypervalency of the phosphorus atom in iminophosphoranes from high-resolution X-ray data and subsequent topological analysis of the multipole refinement. The topological properties are correlated to the results from NMR spectroscopic investigations.

Results and Discussion

Syntheses of 1–4: *N*-(Trimethylsilyl)diphenyl-2-picolyliminophosphorane (**1**) is readily available by the Staudinger reaction of diphenyl-2-picolylphosphane[20] with trimethylsilylazide (Scheme 2). Deprotonation at the methylene bridge of

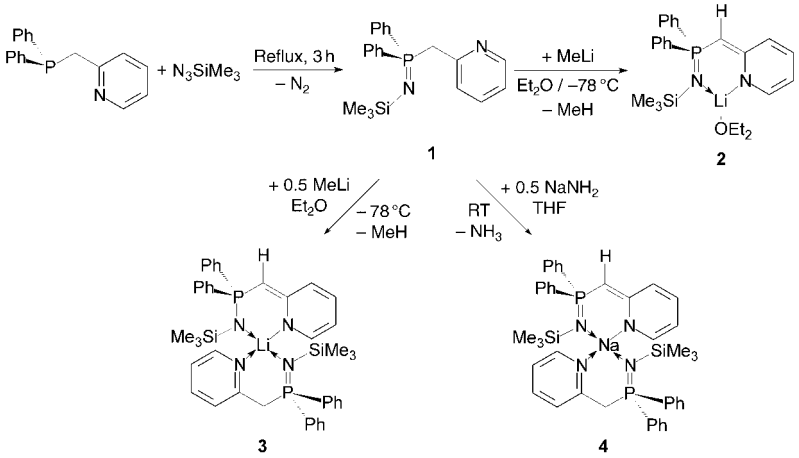

Scheme 2. Synthesis of **1**, deprotonation of **1** with MeLi to give **2** and preparation of **3** and **4**.

Abstract in German: *Das Iminophosphoran $Ph_2P(CH_2Py)(NSiMe_3)$ (**1**), wurde mit Alkalimetallbasen umgesetzt. Die Komplexe $[(Et_2O)Li\{Ph_2P(CHPy)(NSiMe_3)\}]$ (**2**), $[\{Ph_2P(CH_2Py)(NSiMe_3)\}Li\{Ph_2P(CHPy)(NSiMe_3)\}]$ (**3**), und $[\{Ph_2P(CH_2Py)(NSiMe_3)\}Na\{Ph_2P(CHPy)(NSiMe_3)\}]$ (**4**) wurden auf ihr Koordinationsverhalten im Festkörper untersucht. Die NMR-spektroskopischen Eigenschaften in Lösung wurden in Beziehung zum Koordinationsverhalten gesetzt. Darüber hinaus zeigt die experimentelle Elektronendichtebestimmung und die anschließende topologische Analyse, dass zur Beschreibung der Bindungssituation in Iminophosphoranen keine Hypervalenz des Phosphoratoms nötig ist. Die topologischen Eigenschaften des anionischen Liganden in Übereinstimmung mit den NMR-spektroskopischen Ergebnissen zeigen, dass die formale P=N Doppelbindung besser als polare P^+-N^--Einfachbindung zu beschreiben ist. Weiterhin werden Effekte der Metallkoordination auf die Bindungsparameter des Iminophosphorans und seines Anions abgeleitet.*

1 with one equivalent of MeLi in diethyl ether at −78 °C gives the lithium complex $[(Et_2O)Li\{Ph_2P(CHPy)(NSiMe_3)\}]$ (**2**) in high yield. The reaction of only 0.5 equiv of MeLi gives the complex $[\{Ph_2P(CH_2Py)(NSiMe_3)\}Li\{Ph_2P(CHPy)(NSiMe_3)\}]$ (**3**), in which the neutral starting material **1** and the related anion both chelate the same lithium atom. Formally, the diethyl ether donor molecule in **2** is replaced by the iminophosphorane **1**. To obtain insight into the reactivity and coordination flexibility of the ligand, **1** was deprotonated with sodium amide in THF at room temperature. As the neutral donor ligand already proved to be a good bidentate donor in the lithiated complex **3**, the reaction was performed with only 0.5 equiv of $NaNH_2$, so that **1** acted as reagent and donor at the same time, akin to **3**.

Structures: The solid-state structures of the iminophosphorane **1** and the metalated derivatives **2–4** are shown in Figures 1–4, respectively. Selected bond lengths and angles are listed in Table 1; crystallographic details are given in Table 5.

Table 1. Selected bond lengths [pm] and angles [°] of **1**–**4**.

	Anionic ligand				Neutral iminophosphorane		
	2, M = Li	**3**, M = Li	**4**, M = Na		**1**	**3**, M = Li	**4**, M = Na
P1–N1	159.04(2)	158.96(15)	157.79(14)	P2–N3	154.13(12)	156.55(15)	156.28(13)
N1–Si1	170.67(2)	170.69(16)	168.69(14)	N3–Si2	168.08(12)	172.17(15)	172.04(14)
P1–C1	172.57(2)	172.95(19)	173.43(17)	P2–C22	182.57(14)	181.46(19)	183.48(17)
C1–C2	140.13(3)	140.5(3)	141.1(2)	C22–C23	150.39(19)	149.8(3)	150.6(2)
C2–N2	137.07(3)	137.5(2)	137.6(2)	C23–N4	133.17(18)	134.3(2)	134.1(2)
M–N1	194.37(7)	206.9(3)	233.51(15)	M–N3	–	216.5(3)	237.09(14)
M–N2	196.30(7)	209.1(4)	239.16(15)	M–N4	–	210.2(3)	240.00(15)
P1-C1-C2	127.114(19)	123.33(15)	125.42(13)	P2-C22-C23	111.98(9)	119.06(14)	117.95(11)
P1-N1-Si1	130.469(14)	130.67(9)	140.06(9)	P2-N3-Si2	143.91(8)	132.91(9)	130.47(8)
P1–C_{Ph}	av 182.24	av 183.15	av 182.85	P2–C_{Ph}	av 181.67	av 181.91	av 181.63

As expected, the central phosphorus atom in $Ph_2P(CH_2Py)(NSiMe_3)$ (**1**) is tetrahedrally coordinated by three carbon atoms and one nitrogen atom. The P2–C_{Ph} distances (av 181.67 pm) are on average 1 pm shorter than the P2–C22 bond (182.57(14) pm) because of the smaller radius of an sp^2- compared with an sp^3-hybridised carbon atom. The P2–N3 bond length of 154.13(12) pm is in the range normally quoted for a formal P=N double bond in iminophosphoranes (147–162 pm).[3,8,21] As in all N-silyl-substituted iminophosphoranes, the N3–Si2 bond (168.08(12) pm) is considerably shorter than a formal Si–N single bond (174 pm).[22] In the solid-state, **1** adopts a *transoid* conformation in which the two nitrogen atoms N3 of the imino group and N4 of the pyridyl ring point in opposite directions due to repulsion of the N lone pairs. N···H–C hydrogen bonding is not observed (Figure 1).

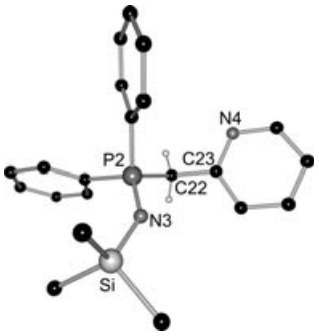

Figure 1. Solid-state structure of **1**; for clarity only the methylene hydrogen atoms are depicted.

Alkali metal complexes tend to form oligomeric aggregates depending on the steric demand of the substituents, the radius and polarisability of the metal atom and the nature and amount of donor solvent.[23] Nevertheless, the above-mentioned reactions of the iminophosphorane **1** with alkali metal deprotonation reagents yielded exclusively monomeric complexes.

In $[(Et_2O)Li\{Ph_2P(CHPy)(NSiMe_3)\}]$ (**2**), the trigonal-planar coordination sphere of the lithium cation is made up of the imino nitrogen atom N1, the pyridyl ring nitrogen atom N2 and the oxygen atom of the diethyl ether donor molecule (Figure 2). The metal cation is displaced by only 22.6 pm from the best plane determined by the three coordinated atoms. As expected from the coordination behaviour,[24] a six-membered metallacycle is formed. The conformation of this ring is a distorted boat arrangement with the deprotonated carbon atom and the metal atom in the bow and stern positions. They lie 29 and 14 pm, respectively, out of the best plane defined by N1-P1-C2-N2.

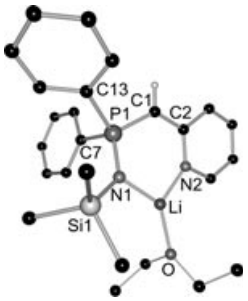

Figure 2. Solid-state structure of **2**; for clarity only the hydrogen atom at the bridging carbon atom is depicted.

The sum of the bond angles at the imino nitrogen atom N1 is very close to 360° indicating a planar environment. The same is valid for the pyridyl ring nitrogen atom N2. In contrast to the chemically related monomeric bis(iminophosphorane)methanides $[(Et_2O)Li\{HC(Cy_2PNSiMe_3)_2\}]$,[25] $[(THF)Li\{HC(Ph_2PNSiMe_3)_2\}]$[26] and the dimeric $[Li\{HC(Ph_2PNSiMe_3)_2\}]_2$,[27] the lithium cation in **2** shows no contact to the deprotonated carbon atom C1 (Li···C1 322.5 pm). The bond angles at C1 are close to 120° and thus indicate sp^2-hybridisation. In contrast to the parent iminophosphorane **1**, N,N-chelation to the metal atom results in a N1/N2 *cisoid* conformation. Remarkably, the Li–N1 distance in **2** (194.37(7) pm) is only slightly shorter than the Li–N2 distance of 196.30(7) pm. Both contacts are at the short end of the range reported for Li–N distances in lithium amides,[28] lithium iminophosphoranates[14a,29] and lithium aminidinates.[30] Metal coordination to N1 elongates the element–nitrogen bonds. Although the P1–N1 bond length in **2** is lengthened by about 5 pm with respect to **1**, it is still in the range generally quoted for formal P=N double bonds in iminophosphoranes.[3,21] Likewise, the N1–Si1 bond (170.67(2) pm) is elongated by 2.7 pm in comparison to the N–Si bond in the iminophosphorane **1**. Similar elongations relative to the related starting materials[31,32] are observed in $[(Et_2O)Li\{(o\text{-}C_6H_4)Ph_2PNSiMe_3\}]_2$[14a] and lithiated bis(iminophosphorane)methanides.[26,27]

Figure 3 shows the solid-state structure of $[\{Ph_2P(CH_2Py)(NSiMe_3)\}Li\{Ph_2P(CHPy)(NSiMe_3)\}]$ (**3**). One deprotonated equivalent of the starting material **1** contributes the monoanionic [N-P-C(H)-Py]$^-$ chelating ligand also present in **2**, while the second equivalent acts as neutral bidentate N,N′-donor base towards the lithium cation.

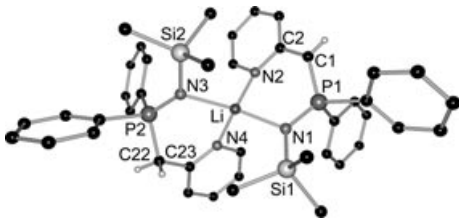

Figure 3. Solid-state structure of **3**; for clarity only the hydrogen atoms at the bridging carbon atoms are depicted.

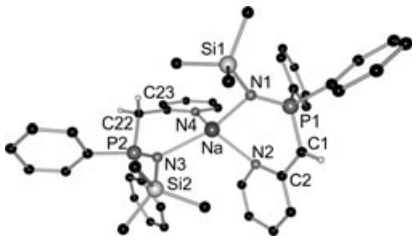

Figure 4. Solid-state structure of **4**; for clarity reasons only the hydrogen atoms at the bridging carbon atoms are depicted.

In **3**, the lithium cation is coordinated in a distorted tetrahedral fashion by the four nitrogen atoms (the N-Li-N angles vary from 98.23(14) to 128.49(17)°). In the metallaspirocycle both six-membered LiN_2C_2P rings adopt a distorted boat conformation. The lithium cation is displaced by 46 pm from the best plane of the anionic ligand, but only 12 pm from the plane of the neutral ligand. As expected, the deprotonated sp^2 carbon atom C1 is closer to the plane than the methylene carbon atom C22 (displacements of 45 and 61 pm, respectively). The Li···C1 distance in **3** is 324.3 pm, that is, 2 pm longer than in **2**. However, due to the more pronounced boat conformation the lithium cation is 16 pm closer to the deprotonated carbon atom C1 than to C22 of the neutral ligand (Li···C22 340.4 pm). The P1-C1-C2 angle of 123.33(15)° indicates sp^2-hybridisation. In the neutral donor ligand, the corresponding angle at C22 of 119.06(14)° is only marginally smaller. The sum of the bond angles at both imino nitrogen atoms N1 and N3 of close to 360° indicates a planar environment. For the pyridyl ring nitrogen atoms N2 and N4, the sum of the angles shows slight displacement of the metal atom from the plane of the heteroaromatic ring (352.2 and 357.7°, respectively). The P1–N1 distances in the anionic ligand of **2** (159.04(2) pm) and **3** (158.96(15) pm) are identical within the ESDs and about 5 pm longer than in the iminophosphorane **1** (154.13(12) pm). The P2–N3 bond length of 156.55(13) pm in the neutral donor ligand in **3** is half-way between them. Interestingly, the N1–Si1 distance of 170.69(16) pm in the anionic ligand of **3** is identical to that in **2**. However, the N2–Si2 distance (172.17(15) pm) is about 1.5 pm longer than in **2** and even 4.1 pm longer than that in the iminophosphorane **1**. Thus, both P–N and N–Si bonds in the anionic and neutral ligand are appreciably elongated on metal coordination at the imino nitrogen atom. As expected from the higher coordination number of the lithium cation and the greater steric bulk of the two ligands, both Li–N bonds in **3** are longer than in **2**. The $Li–N_{imino}$ bond distances in **3** vary remarkably. Whereas the Li–N1 distance to the anion is only 206.9(3) pm, the Li–N3 distance to the donor ligand is 9.6 pm longer. The imino N atom of the anion seems much more attractive to the lithium cation. The $Li–N_{Py}$ distances in **3** differ only by about 1 pm and are in the normal range.[33–35]

The sodium complex $[\{Ph_2P(CH_2Py)(NSiMe_3)\}Na\{Ph_2P(CHPy)(NSiMe_3)\}]$ (**4**) crystallises as yellow blocks from saturated THF solution. The solid-state structure of **4** is depicted in Figure 4. Compounds **3** and **4** are isomorphous but not isostructural.

As in **3** the metal atom is displaced further from the best plane of the anion than from that of the neutral ligand (20 vs 17 pm), and the deprotonated carbon atom is closer to that plane than the methylene carbon atom (34 vs 75 pm). The imino nitrogen atoms N1 and N3 in **4** show trigonal-planar coordination. The same is valid for the pyridyl ring nitrogen atom N4 of the neutral ligand. However, the sum of the angles at the pyridyl ring nitrogen atom N2 in the anionic ligand of 343.4° indicates a displacement of the sodium atom towards the π-electron density of the ring. This more pronounced haptotropic shift of the softer metal atom was observed earlier[36] and is emphasised by the gradual increase in the ordering numbers of the alkali metals.[37] The differences in the P–N bond lengths in the anionic and neutral ligands in **4** are only half as much as in the lithium complex **3**, and the elongation of the formal P=N double bond compared to the starting material **1** is less pronounced. The same is valid for the N–Si distances. The Na–N distances in **4** span the range of 233.51(15) to 240.00(15) pm and are comparable to those of the structurally related monomeric $[(THF)_2Na\{HC(Ph_2PNSiMe_3)_2\}]$[25] (241.6 pm) and dimeric $([Na\{HC(Ph_2PNSiMe_3)_2\}]_2$ (233.4–253.8 pm).[27] The values correspond to those found in sodium amides rather than those in complexes with coordinated amine donor bases such as $[(pmdeta)NaPh]_2$ (260.9–271.2 pm; pmdeta: $MeN(CH_2CH_2NMe_2)_2$).[38] However, the $Na–N_{Py}$ distances are similar to those in, for example, $[(C_5H_5N)_3NaCp^*]$[39] (245.0–248.8 pm; $Cp^* = \eta^5$-C_5Me_5), $[(C_5H_5N)Na\{OtBu(SiMe_2)NSiMe_3\}]$[40] (239.1 pm) and $[(THF)_3Na(PyCPh_2)]$[36] (241.4 pm). Figure 5 depicts a superposition plot of the core structures of the **3** and **4**.

In all compounds **1**–**4** the $P–C_{Ph}$ distances are very similar and do not differ significantly from that of the iminophosphorane **1**. In the iminophosphorane **1** and the neutral ligands in **3** and **4**, the P2–C22 (av 182.5 pm) and C22–C23

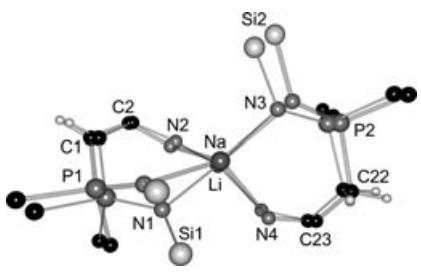

Figure 5. Superposition plot of the core structures of the lithium complex **3** (narrow lines) and the isomorphous sodium complex **4** (wide lines).

(av 150.3 pm) bond lengths are almost equal and are invariant to metal coordination. They are standard P–C (185 pm) and C–C single bonds.[22] However, in the anionic ligands of **2–4**, the average P1–C1 bonds of 173.0 pm are about 10 pm shorter than the corresponding bond in the neutral molecules. In phosphaalkenes, the formal P=C double-bond lengths vary from 161 to 171 pm, and the average value is 167 pm.[41] Ylidic P–C bond lengths lie between 163 and 173 pm,[42] and Gilheany quotes an average value of 169 pm.[7] Thus, the P1–C1 bond lengths in the anionic ligands in this paper suggest partial double-bond character, as depicted in resonance structure **b** of Scheme 3. At the same

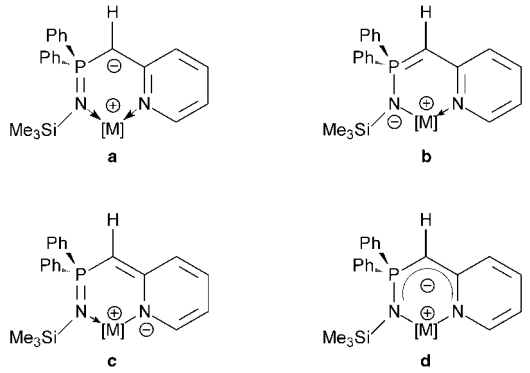

Scheme 3. Resonance forms of $[M\{Ph_2P(CHPy)(NSiMe_3)\}]$: **a** indicates a carbanionic ylidic contribution, **b** shows the amidic ylenic resonance structure, **c** emphasises the amidic olefinic resonance form and **d** visualises the delocalisation of the negative charge.

time, the C1–C2 bonds (av 140.6 pm) are shortened by approximately 10 pm in the anionic versus the neutral ligands, and this reflects a partial double-bond character, as depicted in **c** of Scheme 3.

Furthermore, the fact that the C_{ipso}–N_{Py} bonds of the anionic ligands (av 137.4 pm) are on average 3.5 pm longer than the corresponding bonds in the neutral ligands indicates a perturbation of the aromatic ring system. This might be interpreted as the result of transfer of the negative charge from the deprotonated carbon atom to the pyridyl ring nitrogen atom.

The P–N bond lengths in all isolated compounds are short and range from 154.13(12) pm in **1** to 159.04(2) pm in **2**. Even in the neutral donor ligands of **3** and **4** they are about 2.3 pm longer than in iminophosphorane **1**. In accordance with the harder Lewis-acidic character of the lithium cation in comparison to sodium, the P1–N1 bonds in the lithium complexes **2** (159.04(2) pm) and **3** (158.96(15) pm) are longer than in the sodium derivative **4** (157.79(14) pm). Metal coordination at the imino nitrogen atom of the neutral ligand shifts electron density from the P=N bonding region to the metal, lengthening the P=N bond. Metal coordination at N1 together with deprotonation at the methylene bridge next to the phosphorus atom P1 leads to a further elongation of the P=N bond, as the additional negative carbon atom competes for the charge density of the electropositive phosphorus atom. Charge accumulation at N1 in the anionic ligands furnishes a strong M–N1 interaction, while polarisation of the P2–N3 bond gives a weaker M–N3 bond.

This trend is also reflected in the N–Si bond lengths. In **1**, the shortest N–Si bond (168.08(12) pm) is present. In the anionic ligands of the lithiated complexes **2** and **3**, these bonds are on average 2.6 pm longer than in the iminophosphorane **1**. In **4**, it is very similar to the distance in **1**, that is, the softer sodium atom is less polarising towards the anionic ligand. In comparison with standard N–Si single bonds (174 pm)[22] they all are inherently short. Interestingly, the N3–Si2 distances in the neutral ligands of **3** and **4** are about 4 pm longer than in the iminophosphorane **1** and are therefore almost in the range of standard N–Si single bonds. In the iminophosphorane **1**, the negatively polarised imino nitrogen atom N3 is bonded to the electropositive phosphorus and silicon atoms. These interactions result in a short N3–Si2 bond in **1**. On metal coordination at N3, the negatively polarised imino nitrogen atom has a further interaction with the cationic centre. Thus, the N3–Si2 distances in **3** and **4** become longer. In the anionic ligands of **2–4** the N1–Si1 bond lengths are half-way between that in **1** and those of the neutral ligands in **3** and **4**. The negatively polarised imino nitrogen atom N1 interacts with the cation, the electropositive silicon atom and a less electropositive phosphorus centre, due to the neighbouring negatively polarised deprotonated carbon atom C1. Thus, the N–Si distances are longer than in iminophosphorane **1**, but shorter than in the neutral ligands of **3** and **4**.

In conclusion, all the geometrical features of the anionic ligands in the metalated complexes **2–4** suggest canonical formulas as depicted in Scheme 3. However, all of them require valence expansion at the phosphorus atom, at variance with the eight-electron rule, but chemical reactivity supports neither P=N nor P=C double bonds, because both are easily cleaved in various reactions.[14]

NMR spectroscopic investigations: To elucidate the charge distribution in **1–4**, we performed several NMR experiments in solution. The chemical shifts determined for the ^{31}P and ^{15}N nuclei are summarised in Table 2.

Table 2. ^{31}P and ^{15}N NMR shifts [ppm] of **1–4**.

	Anionic ligands			Neutral ligands		
	P	N_{imino}	N_{Py}	P	N_{imino}	N_{Py}
1	–	–	–	−0.32	−343	−61
2	18.03	−331	−145	–	–	–
3	15.36	−334	−139	8.46	−339	−68
4	11.30	−345	−137	−0.60	−332	−63

Deprotonation at the C_α-atom in the iminophosphorane $Ph_2P(CH_2Py)(NSiMe_3)$ (**1**) results in ^{31}P NMR downfield shifts relative to **1** and the neutral ligands in **3** and **4**. This shift seems to be counterintuitive to the idea of P=C bond generation in the anions.

An interesting result was obtained in the $^{1}H,^{15}N$ HMBC NMR experiments. In the starting material **1** and in the neutral ligands of **3** and **4**, the pyridyl nitrogen atoms resonate at similar frequencies ($\delta = -61$ to -68). The observed small

differences arise from metal coordination at the ring nitrogen atom. Remarkably, they reflect the polarising abilities of the metal, and hence the upfield shift due to sodium coordination is less pronounced than the changes induced by the lithium cation. However, the ^{15}N NMR signals for the pyridyl ring nitrogen atoms in the anionic ligands are considerably shifted to higher fields ($\delta = -137$ to -145) with respect to **1** ($\delta = -61$) and to the neutral ligands in **3** and **4**. These NMR spectroscopic shifts can be explained by a considerable charge transfer from the carbanionic atom C1 to the heteroaromatic ring and accumulation at the pyridyl nitrogen atom. Additionally, the almost invariant ^{15}N NMR shift of the imino nitrogen atom in all compounds indicates that the charge density at this nitrogen atom is less affected by deprotonation.

Charge transfer to the pyridyl substituent in the anionic ligands of **2**–**4** is also evident from the ^{1}H and ^{13}C NMR spectroscopic experiments. In Table 3, these chemical shifts are compared with those of the starting material **1** and the neutral ligands in **3** and **4**. Deprotonation at C_α in iminophosphorane **1** results in a upfield shift for the pyridyl hydrogen atoms relative to the corresponding atoms in the neutral ligands of **3** and **4** and the parent iminophosphorane **1**. The charge density is accumulated in the pyridyl substituent. In the ^{13}C NMR spectrum, the deprotonated C1 atoms in the anionic ligands resonate at lower fields compared to the neutral ligands. Additionally, the carbon atom atoms adjacent to the ring nitrogen atoms are shifted downfield.

However, in quintessence neither the geometrical parameters from the structure determination nor the NMR spectroscopic data provide a conclusive criterion to decide which resonance form in Scheme 3, if any, contributes most to the bonding in alkali metal complexes **1**–**4**.

Charge-density distribution in [(Et_2O)Li{Ph_2P(CHPy)(N-$SiMe_3$)}] (2): To describe the charge-density distribution in [(Et_2O)Li{Ph_2P(CHPy)($NSiMe_3$)}] (**2**), we performed a multipole refinement based on the formalism of Hansen and Coppens[43] with 100 K high-resolution data up to $(\sin\theta/\lambda)_{max} = 1.145$ Å^{-1}. The results of the topological analysis are presented in terms of the charge density $\rho(\boldsymbol{r})$, the Laplacian $\nabla^2\rho(\boldsymbol{r})$ and the charges obtained from the integration over the atomic basins according to Bader's theory of atoms in molecules (AIM).[44] All bond critical points (BCPs) at the P–E bonds are displaced towards the electropositive phosphorus atom. A comparison of the densities $\rho(\boldsymbol{r}_{BCP})$, the algebraic sum of the eigenvalues λ_i of the Hessian matrix $\nabla^2\rho(\boldsymbol{r}_{BCP})$ of these bonds and the integrated charges are presented in Table 4.

Table 4. Topology of the P–N and P–C bonds in **2**.[a]

A–B	d(A–B)	d(A–BCP)	d(BCP–B)	$\rho(\boldsymbol{r}_{BCP})$	$\nabla^2\rho(\boldsymbol{r}_{BCP})$	Charge at B
P–N1	1.5903	0.6566	0.9337	1.508(10)	5.874(28)	−1.98
P–C1	1.7252	0.7753	0.9499	1.336(8)	−8.325(22)	−0.54
P–C7	1.8294	0.8047	1.0248	1.134(6)	−6.402(15)	−0.31
P–C13	1.8147	0.7784	1.0364	1.151(8)	−6.145(16)	−0.34

[a] d(A–B): distance [Å] between atoms A and B along the bond path; d(A–BCP), d(BCP–B): distance between the BCP and atoms A and B, respectively; $\rho(\boldsymbol{r}_{BCP})$: charge density [e Å^{-3}] at the BCP; $\nabla^2\rho(\boldsymbol{r}_{BCP})$: Laplacian of $\rho(\boldsymbol{r})$ at the BCP [eÅ^{-5}]; Charges of B from integration over atomic basins in electrons, charge of the phosphorus atom A: +2.20.

The properties at the BCPs of the aromatic C–C bonds in the phenyl rings and those in the $SiMe_3$ group are in the expected range. The two topologically analysed P–C_{Ph} bonds in **2** are comparable to those in the triphenylphosphane ligand of a transition metal complex.[45] In contrast to the P–C_{Ph} bonds in triphenylphosphonium benzylide Ph_3P=C(H)Ph, no variance in the topology between the two P–C_{Ph} bonds in **2** could be observed.[12] Compared to the latter, the P–C1 bond displays higher charge density and a more negative Laplacian at the BCP. An inspection of the Laplacian along the P–C bond paths (Figure 6) in **2** reveals an almost equal charge distribution in the phosphorus basin, while the main difference concerning the Laplacian in the basin of the carbon atoms is related to the shorter distance between C1 and BCP_{P-C1}. This rather short P–C bond results from distinct electrostatic interactions between the negatively polarised deprotonated C1 and the electropositive phosphorus atom, as reflected in the charges of −0.52 e for C1 and +2.20 e for P from integration over the atomic basins.[46]

The properties of the exocyclic C1–C2 bond, which are almost the same as those of an aromatic C–C bond, as well as the aromatic character of the C2–N2 bond of the pyridine ring fuels the idea of delocalisation of the negative charge in the C1-C2-N2 residue. This exocyclic delocalisation slightly

Table 3. Selected ^{1}H and ^{13}C NMR shifts [ppm] of **1**–**4**.

	^{1}H					^{13}C					
	1	3	4	5	6	1	2	3	4	5	6
1	3.56	7.18	7.07	6.55	8.28	43.2	152.3	125.6	129.5	121.6	149.6
2	3.58	6.42	6.71	5.77	7.12	55.8	167.8	118.9	134.8	106.9	147.5
3a[a]	4.11	6.60	7.00	5.95	7.33	59.0	166.3	118.4	134.2	103.6	148.0
3b[a]	3.78	6.85	7.00	6.42	8.46	39.7	150.7	126.6	128.3	121.5	152.2
4a[a]	3.39	6.18	6.64	5.51	7.15	58.2	168.0	117.9	133.5	103.9	147.8
4b[a]	3.85	7.15	7.44	6.98	8.31	42.5	155.3	125.8	131.1	122.1	149.8

[a] **a**: anionic ligand, **b**: neutral ligand.

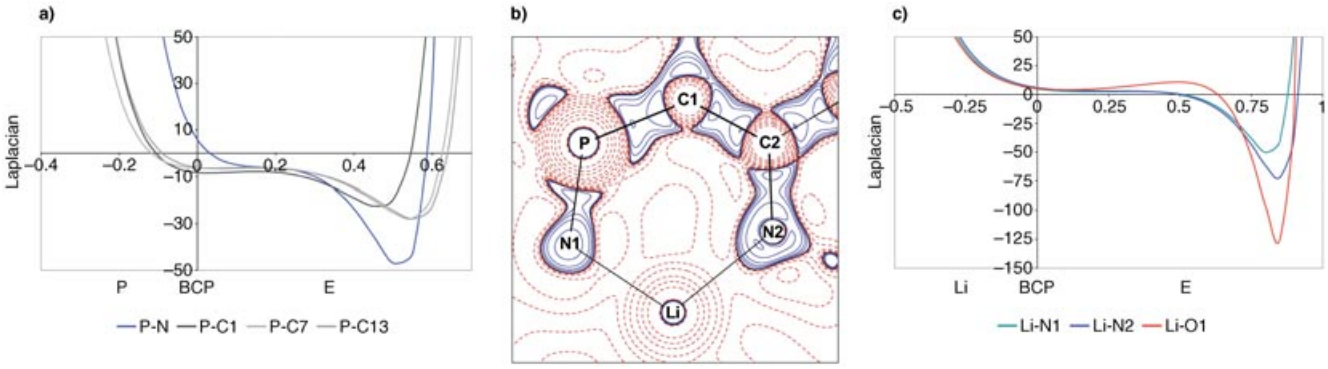

Figure 6. a) Laplacian along the bond paths of the P–C and P–N bonds; b) Laplacian in the P1-C2-Li plane (blue lines indicate charge concentrations, red lines indicate charge depletions); c) Laplacian along the bond paths of the Li–N and Li–O bonds. The zero value of the x axis indicates the position of the BCP.

perturbs the aromaticity of the heteroaromatic ring. The bond lengths and electron densities in the pyridyl substituent differ from those in undisturbed rings.[47]

The Laplacian distribution $\nabla^2\rho(\boldsymbol{r})$ along the P–N1 bond is completely different to that of the P–C_{ipso} bonds. The Laplacian at the BCP is positive and charge density is exclusively concentrated in the nitrogen basin (Figure 6a). This indicates a severe contribution of electrostatic interaction to the bonding energy, further substantiated by the integration of the atomic basins.[46] The two basins related to the nitrogen atoms give distinct negative values. The imino nitrogen atom N1 is bonded to three electropositive neighbours, and therefore the charge of −1.91 e is higher than that of −1.11 e for the ring nitrogen atom N2. The charge of the deprotonated carbon atom C1 is about 0.2 e higher than those of the two phosphorus bonded *ipso* carbon atoms (C7: −0.30 e, C13: −0.34 e). All these findings support an ylidic P^+–C^- simultaneous with a P^+–N^- bond, not yet present in the resonance forms of Scheme 3. The determination of the (3;−3) critical points in the spatial distribution of $-\nabla^2\rho(\boldsymbol{r})$ and quantification of the valence shell charge concentrations (VSCCs) around the electronegative atoms (N1, N2, O1, C1) confirms this view. Isosurface presentations around N1 and a contour plot in the plane containing the (3;−3) critical points are presented in Figure 7a. They indicate sp^3-hybridisation at N1 with two lone pairs, both oriented towards the Li cation. The same is valid for O1 (Figure 7b). The angle between the lone pairs LP1-N1-LP2 of approximately 71° is much more acute than the expected 109°, but can be rationalised by the closer approach of the critical points by simultaneous interaction of both VSCCs with the lithium cation. Clearly, the lone pairs at N1 and O1 act as a bifurcated donor to the electropositive metal acceptor. We found the same arrangement at S-bonded sp^3-hybridised nitrogen atoms in an intramolecular hydrogen bond.[48]

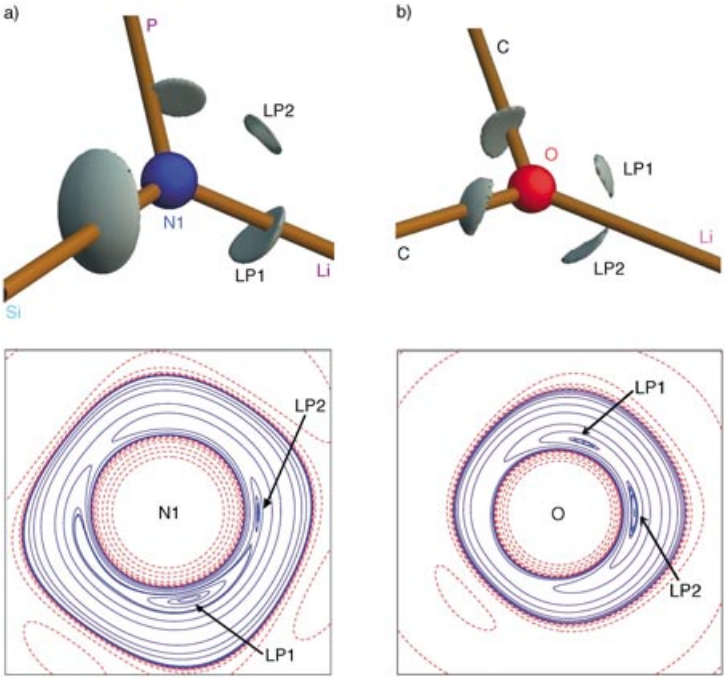

Figure 7. Isosurface maps at constant $\nabla^2\rho(\boldsymbol{r})$ values indicating bonding and nonbonding charge concentrations around the displayed atoms, and contour plots in a plane with the two lone pairs oriented towards Li1 for N1 (a) and O1 (b) in **2**; a) N1, $\nabla^2\rho(\boldsymbol{r}) = -48$ e Å^{-5} (bonding VSCCs) and −41 e Å^{-5} (nonbonding VSCCs); b) O1, $\nabla^2\rho(\boldsymbol{r}) = -125$ e Å^{-5} (bonding VSCCs) and −105 e Å^{-5} (nonbonding VSCCs). Blue contours indicate charge concentration, and red contours charge depletion.

Conclusion

The experimental charge-density distribution in [(Et_2O)-Li{$Ph_2P(CHPy)(NSiMe_3)$}] (**2**) clearly proves that the formal P=N imino double bond and the potential ylenic P=C double bond must be written as polar P^+–N^- and P^+–C^- single bonds augmented by electrostatic contributions. As predicted from calculations, a hypervalent central phosphorus atom is not required to describe the bonding. It is much more appropriate to assign charges in the resonance formula, even for the starting material $Ph_2P(CH_2Py)(NSiMe_3)$ (**1**). The almost invariant imino nitrogen signals in the ^{15}N NMR spectra of **1**–**4** further supplies credibility to these canonical forms. The iminophosphorane **1** is better been written as a zwitterionic phosphonium amide $Ph_2(PyCH_2)P^+$–$^-NSiMe_3$.

This polar single bond corresponds best with the reactivity: metal organyls in polar solvents can more easily cleave

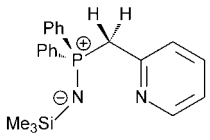

1

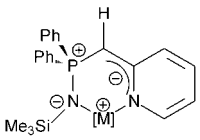

2–4

this bond rather than the wrongly assigned P=N double bond. Therefore, deimination or the retro-Staudinger reaction of iminophosphoranes seems an unorthodox but suitable synthetic route to phosphanes.

The isolation of the complexes [{$Ph_2P(CH_2Py)(NSiMe_3)$}M{$Ph_2P(CHPy)(NSiMe_3)$}] (M = Li: **3**, Na: **4**), in which both anionic and neutral iminophosphorane are bound to the cation, allowed a detailed discussion of the geometrical parameters in the ligands and we were able to deduce the effects of metal coordination on the structural parameters of the neutral iminophosphorane and its anionic derivative. The electrostatic contributions to the P–N bonding and the negatively charged imino nitrogen atom result in short P–N and N–Si distances in iminophosphorane **1**. The negative charge at the imino nitrogen atom in **1** is stabilised by the positive phosphorus centre and the electropositive silicon atom, and this results in short P–N and N–Si contacts. The observed elongations of these bonds in the neutral metal-coordinating ligands are a result of polarisation of the negative charge by the cations. The elongation of the P–N distances found in the anionic ligands are explained by the interaction of the positively charged phosphorus centre with the negatively polarised C_α atom, which weakens the electrostatic contribution to the P–N bonds.

Experimental Section

All reactions were performed under an inert atmosphere of dry N_2 with Schlenk techniques or in an argon glove box. All solvents were dried over Na/K alloy and distilled prior to use. NMR spectra were recorded at room temperature on a Bruker DRX 300 spectrometer at 300.1 (^{1}H), 75.5 (^{13}C), 121.5 (^{31}P), 59.6 (^{29}Si), 155.5 (^{7}Li), 79.4 (^{23}Na) and 30.4 MHz (^{1}H,^{15}N HMBC). Chemical shifts δ are relative to the solvent for ^{1}H, ^{13}C and ^{1}H,^{15}N HMBC NMR, to H_3PO_4 (85%) for ^{31}P, to external saturated LiCl solution for ^{7}Li, to 0.1 M NaCl in D_2O for ^{23}Na and to $SiMe_4$ for ^{29}Si NMR. Elemental analyses were performed by the Microanalytisches Labor der Universität Würzburg.

The NMR shifts were assigned according to the following scheme:

The heteronuclei are assigned an asterisk in the neutral ligands of compounds **3** and **4**.

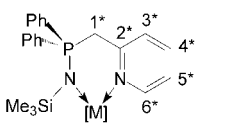

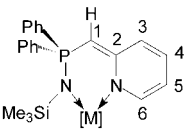

$Ph_2P(CH_2Py)(NSiMe_3)$, (1): N_3SiMe_3 (0.46 g, 3.97 mmol) was added to Ph_2PCH_2Py (1.00 g, 3.61 mmol). The reaction mixture was heated under reflux for 3 h. Evaporation of the excess of N_3SiMe_3 and distillation of the crude product under vacuum gave pure $Ph_2P(CH_2Py)(NSiMe_3)$ (**1**; 1.29 g, 3.53 mmol, 98%) as a colourless oil. Addition of hexane to the oil and storage at −16 °C gave **1** as colourless plates. M.p. (DTA): 44 °C; ^{31}P NMR ([D$_8$]toluene): $\delta = -0.32$ (s); ^{29}Si NMR ([D$_8$]toluene): $\delta = -10.61$ (s); ^{1}H,^{15}N HMBC ([D$_8$]toluene): $\delta = -343$ (s, $NSiMe_3$), −61 (s, pyN); ^{1}H NMR ([D$_8$]toluene): $\delta = 0.23$ (s, 9H, $SiMe_3$), 3.56 (d, $^2J_{PH} = 14.1$ Hz, 2H, H1), 6.55 (dddd, 1H, H5), 7.07 (m, 1H, H4), 7.18 (d, 1H, H3), 8.28 (d, 1H, H6), 7.00–7.05 (m, 6H, *m*-, *p*-PhH), 7.65–7.81 (m, 4H, *o*-PhH); ^{13}C NMR ([D$_8$]toluene): $\delta = 4.8$ (d, $^3J_{SiC} = 3.0$ Hz, $SiMe_3$), 43.2 (d, C1), 121.6 (d, C5), 125.6 (d, C3), 129.5 (d, C4), 149.6 (d, C6), 152.3 (d, C2), 129.2 (*m*-PhC), 131.0 (*p*-PhC), 131.8 (*o*-PhC), 134.9 (*ipso*-PhC); elemental analysis (%) calcd for $C_{21}H_{25}N_2PSi$: C 69.44, H 7.68, N 7.36; found: C 69.24, H 7.72, N 7.43.

[$(Et_2O)Li\{Ph_2P(CHPy)(NSiMe_3)\}$] (2): Compound **1** (0.50 g, 1.37 mmol) was dissolved in Et_2O (10 mL) and cooled to −78 °C. To this solution MeLi (0.94 mL, 1.6 M in Et_2O, 1.51 mmol) was added dropwise. After warming to RT and stirring the yellow solution for 2 h the volume of the solvent was reduced. After 48 h crystalline **2** (0.48 g, 1.08 mmol, 79%) was isolated. M.p. (DTA): 104 °C; ^{31}P NMR ([D$_8$]toluene): $\delta = 18.03$ (s); ^{7}Li NMR ([D$_8$]toluene): $\delta = 1.50$ (s); ^{29}Si NMR ([D$_8$]toluene): $\delta = -8.63$ (s); ^{1}H,^{15}N HMBC NMR ([D$_8$]toluene): $\delta = -331$ ($NSiMe_3$), −145 (pyN); ^{1}H NMR ([D$_8$]toluene): $\delta = 0.11$ (s, 9H, $SiMe_3$), 3.58 (d, $^2J_{PH} = 18.2$ Hz, 1H, H1), 5.77 (dd, 1H, H5), 6.42 (d, 1H, H3), 6.71 (dd, 1H, H4), 7.12 (d, 1H, H6), 7.01–7.06 (m, 6H, *m*-,*p*-PhH), 7.79–7.82 (m, 4H, *o*-PhH), 3.08 (q, 4H, OCH_2CH_3), 0.93 (t, 6H, OCH_2CH_3); ^{13}C NMR ([D$_8$]toluene): $\delta = 4.9$ (d, $^3J_{SiC} = 3.8$ Hz, $SiMe_3$), 55.8 (d, C1), 106.9 (s, C5), 118.9 (d, C3), 134.8 (d, C4), 147.5 (s, C6), 167.8 (d, C2), 128.8 (*m*-PhC), 130.3 (*p*-PhC), 132.5 (*o*-PhC), 137.4 (*ipso*-PhC); elemental analysis (%) calcd for $C_{25}H_{34}LiN_2OPSi$: C 67.54, H 7.71, N 6.30 found: C 67.42, H 7.72, N 6.38.

[{$Ph_2P(CH_2Py)NSiMe_3$}$Li\{Ph_2P(CHPy)NSiMe_3\}$] (3): Compound **1** (0.50 g, 1.37 mmol) was dissolved in Et_2O (30 mL) and cooled to −78 °C. To this solution MeLi (0.43 mL, 1.6 M in Et_2O, 0.69 mmol) was added dropwise. After warming to RT and stirring for 8 h the clear yellow solution was allowed to stand at RT for 3 d to yield **3** (0.80 g, 1.08 mmol, 79%) as yellow blocks. M.p. (DTA): 77 °C (decomp); ^{31}P NMR ([D$_6$]benzene): $\delta = 8.46$ (brs, P*), 15.36 (s, P); ^{7}Li NMR ([D$_6$]benzene): $\delta = 1.70$ (s); ^{1}H, ^{29}Si HMBC NMR ([D$_6$]benzene): $\delta = -9.5$ (s, Si), −1.82 (s, Si*); ^{1}H,^{15}N HMBC NMR ([D$_6$]benzene): $\delta = -339$ (Me_3SiN*), −334 (Me_3SiN), −139 (PyN), −68 (PyN*); ^{1}H NMR ([D$_6$]benzene): $\delta = 0.39$ (s, 9H, $SiMe_3$*), 0.50 (s, 9H, $SiMe_3$), 3.78 (d, $^2J_{PH} = 13.9$ Hz, 2H, H1*), 4.11 (d, $^2J_{PH} = 23.6$ Hz, 1H, H1), 5.95 (dd, 1H, H5), 6.42 (dd, 1H, H5*), 6.60 (d, 1H, H3), 6.85 (d, 2H, H3*), 7.00 (m, 2H, H4, H4*), 7.33 (d, 1H, H6), 8.46 (d, 1H, H6*), 7.25–7.30 (m, 6H, *m*-, *p*-PhH), 7.21–7.24 (m, 6H, *m*-, *p*-PhH*), 7.52–7.70 (m, 4H, *o*-PhH*), 8.08–8.25 (m, 4H, *o*-PhH); ^{13}C NMR ([D$_6$]benzene): $\delta = 2.9$ (d, $^3J_{SiC} = 4.5$ Hz, $SiMe_3$*), 3.8 (d, $^3J_{SiC} = 4.5$ Hz, $SiMe_3$), 39.7 (d, C1*), 59.0 (d, C1), 103.6 (s, C5), 118.4 (d, C3), 121.5 (d, C5*), 126.6 (s, C3*), 128.3 (d, C4*), 134.2 (d, C4), 148.0 (s, C6), 150.7 (s, *ipso*-PyC*), 152.2 (s, C6*), 166.3 (s, *ipso*-PyC), 128.3 (*m*-PhC), 128.5 (*m*-PhC*), 129.8 (*p*-PhC), 130.7 (*p*-PhC*), 131.4 (*o*-PhC*), 132.8 (*o*-PhC), 137.7 (*ipso*-PhC), 138.5 (*ipso*-PhC*); elemental analysis (%) calcd for $C_{42}H_{49}LiN_4P_2Si_2$: C 68.64, H 6.72, N 7.62 found: C 69.01, H 6.52, N 7.73.

[{$Ph_2P(CH_2Py)NSiMe_3$}$Na\{Ph_2P(CHPy)NSiMe_3\}$] (4): A suspension of $NaNH_2$ (0.11 g, 2.75 mmol) in THF (5 mL) was added to a solution of **1** (2.00 g, 5.49 mmol) in THF (40 mL) at RT. After 3 d, the yellow reaction mixture was filtered and the volume of the solution was reduced by evaporation. Storage of the clear yellow solution at RT for several days gave **4** (3.05 g, 4.06 mmol, 74%) as yellow blocks. M.p. (DTA): 33 °C (decomp); ^{31}P NMR ([D$_8$]THF): $\delta = -0.6$ (brs, P*), 11.3 (brs, P); ^{23}Na NMR ([D$_8$]THF): $\delta = 5.02$ (brs); ^{29}Si NMR ([D$_8$]THF): $\delta = -13.9$ (d, $^2J_{SiP} = 8.3$ Hz, Si), −12.8 (d, $^2J_{SiP} = 23.3$ Hz, Si*); ^{1}H,^{15}N HMBC NMR ([D$_8$]THF): $\delta = -345$ (Me_3SiN*), −332 (Me_3SiN), −137 (PyN), −63 (PyN*); ^{1}H NMR ([D$_8$]THF): $\delta = -0.14$ (s, 9H, $SiMe_3$*), −0.20 (s, 9H, $SiMe_3$), 3.39 (d, $^2J_{PH} = 22.3$ Hz, 1H, H1), 3.85 (d, $^2J_{PH} = 14.1$ Hz, 2H, H1*), 5.51 (dd, 1H, H5), 6.18 (d, 1H, H3), 6.64 (dd, 1H, H4), 6.98 (dd, 1H, H5*), 7.14–7.17 (m, 2H, H6, H3*), 7.18–7.25 (m, 8H, *m*-, *p*-PhH, *p*-PhH*), 7.44 (dd, 1H, H4*), 7.69–7.77 (m, 8H, *o*-PhH, *o*-PhH*), 7.31–7.38 (m, 4H, *m*-PhH*), 8.31 (d, 1H, H6*); ^{13}C NMR ([D$_8$]THF): $\delta = 3.87$ (d, $^3J_{SiC} = 4.5$ Hz, $SiMe_3$), 3.69 (d, $^3J_{SiC} = 3.0$ Hz, $SiMe_3$*), 42.5 (d, C1*), 58.2 (d, C1), 103.9 (s, C5), 117.9 (d, C3), 122.1 (d, C5*), 125.8 (d, C3*), 131.1 (d, C4*), 133.5 (d, C4), 147.8 (s, C6), 149.8 (d, C6*), 155.3 (d, *ipso*-PyC*),168.0 (d, *ipso*-PyC), 128.2 (*m*-, *p*-PhC), 128.8 (*m*-PhC*), 129.5 (*p*-PhC*), 132.0 and 132.8 (*o*-PhC, *o*-PhC*), 137.3 (*ipso*-PhC*), 141.3 (*ipso*-

PhC); elemental analysis (%) calcd for $C_{42}H_{49}N_4P_2Si_2$: C 67.17, H 6.58, N 7.46 found: C 66.36, H 6.70, N 7.21.

Structure determination of 1–4: Crystallographic data for **1–4** are listed in Table 5. All data were measured at low temperature[49] with graphite-monochromated $Mo_{K\alpha}$ radiation ($\lambda = 71.073$ pm) on a Bruker D8 goniometer platform, equipped with a Smart Apex CCD detector. Cell parameters were determined and refined using the SMART software.[50] Series of ω scans were performed at several ϕ settings. Raw frame data were integrated using the SAINT program.[51] The structures were solved using direct methods and refined by full-matrix least-squares techniques on F^2 using SHELXTL.[52] Data of **1** and **2** were subjected to empirical correction for absorption with SADABS2.[53] The hydrogen atoms H1 at C1 in **2**, H1 at C1 and H22A, H22B at C22 in **3** and **4** were taken from the difference Fourier map and refined freely. All other hydrogen atoms were refined using a riding model. The U_{iso} values for the hydrogen atoms of a CH_3 group were set to 150%, and those of all other hydrogen atoms to 120%, of the U_{eq} values of the corresponding C atoms. All non-hydrogen atoms were refined anisotropically. The anisotropic displacement parameters (ADPs) in the Supporting Information were plotted at the 50% probability level.

CCDC-231738–231741 contain the supplementary crystallographic data for this paper. These data can be obtained free of charge via www.ccdc.cam.ac.uk/conts/retrieving.html (or from the Cambridge Crystallographic Data Centre, 12 Union Road, Cambridge CB21EZ, UK; fax: (+44) 1223-336-033; or deposit@ccdc.cam.uk).

Table 5. Crystallographic data for compounds **1–4**.

	1	**2**[a]	**3**	**4**
formula	$C_{21}H_{25}N_2PSi$	$C_{25}H_{34}LiN_2OPSi$	$C_{42}H_{49}LiN_4P_2Si_2$	$C_{42}H_{49}N_4NaP_2Si_2$
M_r [g mol^{-1}]	364.49	444.54	734.91	750.96
CCDC no.	231738	231739	231740	231741
T [K]	173(2)	100(2)	100(2)	173(2)
crystal system	triclinic	triclinic	triclinic	monoclinic
space group	$P\bar{1}$	$P\bar{1}$	$P\bar{1}$	$P2_1/n$
a [pm]	905.67(5)	1038.40(2)	1011.46(6)	1124.06(18)
b [pm]	1064.73(6)	1047.83(2)	1104.73(7)	1488.1(2)
c [pm]	1145.95(6)	1285.27(2)	1825.93(11)	2478.7(4)
α [°]	97.0510(10)	73.07°	93.3760(10)	
β [°]	99.3490(10)	81.05°	93.6010(10)	101.283(3)
γ [°]	107.1020(10)	67.66°	98.7470(10)	
V [nm^{-3}]	1.02496(10)	1.23586(4)	2.0077(2)	4.0661(11)
Z	2	2	2	4
ρ_{calcd} [Mgm^{-3}]	1.181	1.195	1.216	1.227
μ [mm^{-1}]	0.198	0.18	0.203	0.211
$F(000)$	388	476	780	1592
crystal size [mm]	0.4×0.4×0.05	0.60×0.57×0.55	0.4×0.4×0.35	0.4×0.4×0.4
θ range [°]	1.83–26.37	1.66–54.54	2.11–26.41	3.05–26.37
reflns collected, low batch	13417	51465[b]	22724	87301
reflns collected, high batch	–	74909[c]	–	–
independent reflns (R_{int}), low batch	4165 (0.0189)	5045 (0.0246)	8174 (0.0400)	8675 (0.0950)
independent reflns (R_{int}), high batch	–	25005 (0.0269)	–	–
absorption correction	empirical	empirical	none	none
max/min transmission	0.98/0.91	0.99/0.95	–	–
data/restraints/parameters	4165/0/229	30050/0/384	8170/0/478	8300/0/478
GOF on F^2	1.051	1.048	0.922	1.086
final R indices [$I > 2\sigma(I)$]				
$R1$	0.0343	0.0298	0.0410	0.0414
$wR2$	0.0940	0.0899	0.0859	0.1150
R indices (all data)				
$R1$	0.0389	0.0378	0.0581	0.0482
$wR2$	0.0973	0.0956	0.0890	0.1188
largest diff. peak/hole [e nm^{-3}]	336/−196	695/−285	479/−360	813/−276

[a] For the sake of comparison, the data of the conventional IAM refinement are given in this table. For the results of the multipole refinement of ED, see Supporting Information. [b] $\sin\theta/\lambda < 0.625$ Å^{-1}. [c] $0.625 < \sin\theta/\lambda < 1.145$ Å^{-1}.

Acknowledgement

This work was supported by the Deutsche Forschungsgemeinschaft (grant no. Sta 334/8-3 and Graduiertenkolleg 690 *Elektronendichte—Theorie und Experiment*) and Chemetall, Frankfurt/Main.

[1] G. Wittig, G. Geissler, *Justus Liebigs Ann. Chem.* **1953**, *580*, 44.
[2] H. Staudinger, J. Meyer, *Helv. Chim. Acta* **1919**, *2*, 635.
[3] A. W. Johnson, *Ylides and Imines of Phosphorus*, Wiley, New York, **1993**.
[4] Review: K. Dehnicke, F. Weller, *Coord. Chem. Rev.* **1997**, *158*, 103.
[5] Review: K. Dehnicke, M. Krieger, W. Massa, *Coord. Chem. Rev.* **1999**, *182*, 19.
[6] a) R. E. v. H. Spence, S. J. Brown, R. P. Wurz, D. Jeremic, D. W. Stephan, *PCT Int. Appl.* WO 2000-CA978 20000824, CA 99-2282070D, **2001**; b) W. Stephan, J. C. Stewart, F. Guerin, S. Courtenay, J. Kickham, E. Hollink, C. Beddie, A. Hoskin, T. Graham, P. Wie, R. E. v. H. Spence, W. Xu, L. Koch, X. Gao, D. G. Harrison, *Organometallics* **2003**, *22*, 1937.
[7] Review: D. G. Gilheany, *Chem. Rev.* **1994**, *94*, 1339.
[8] a) Review: A. Steiner, S. Zacchini, P. I. Richards, *Coord. Chem. Rev.* **2002**, *227*, 193; b) J. F. Bickley, M. C. Copsey, J. C. Jeffery, A. P. Leedham, C. A. Russell, D. Stalke, A. Steiner, T. Stey, S. Zacchini, *J. Chem. Soc. Dalton Trans.* **2004**, 989.
[9] a) W. Kutzelnigg, *Angew. Chem.* **1984**, *96*, 262; *Angew. Chem. Int. Ed. Engl.* **1984**, *23*, 272; b) E. A. Reed, P. v R. Schleyer, *J. Am. Chem. Soc.* **1990**, *112*, 1434; c) E. J. Magnusson, *J. Am. Chem. Soc.* **1993**, *115*, 1051; d) A. Dobado, H. Martinez-García, J. M. Molina, M. R. Sundberg, *J. Am. Chem. Soc.* **1998**, *120*, 8461; e) D. B. Chesnut, *J. Phys. Chem. A* **2003**, *107*, 4307.
[10] a) T. Naito, S. Nagase, H. Yamataka, *J. Am. Chem. Soc.* **1994**, *116*, 10080; b) A. A. Restrepo-Cossio, C. A. Gonzalez, F. Mari, *J. Phys. Chem. A* **1998**, *102*, 6993; c) H. Yamataka, S. Nagase, *J. Am. Chem. Soc.* **1998**, *120*, 7530; d) J. A. Doblado, H. Martinez-Garcia, J. M. Molina, M. R. Sundberg, *J. Am. Chem. Soc.* **2000**, *122*, 1144.
[11] a) W. C. Lu, C. B. Liu, C. C. Sun, *J. Phys. Chem. A* **1999**, *103*, 1078; b) C. W. Lu, C. C. Sun, Q. J. Zang, C. B. Liu, *Chem. Phys. Lett.* **1999**, *311*, 491; c) J. Koketsu, Y. Ninomiya, Y. Suzuki, N. Koga, *Inorg. Chem.* **1997**, *36*, 694.
[12] D. S. Yufit, J. A. K. Howard, M. G. Davidson, *J. Chem. Soc. Perkin Trans. 2* **2000**, 249.
[13] a) G. Fries, J. Wolf, M. Pfeiffer, D. Stalke, H. Werner, *Angew. Chem.* **2000**, *112*, 575; *Angew. Chem. Int. Ed.* **2000**, *39*, 564; b) L. Mahalakshmi, D. Stalke in *Structure and Bonding—Group 13 Chemistry I* (Eds.: D. A. Atwood, H. W. Roesky), Springer, Heidelberg, **2002**, *103*, p. 85.
[14] a) A. Steiner, D. Stalke, *Angew. Chem.* **1995**, *107*, 1908; *Angew. Chem. Int. Ed. Engl.* **1995**, *34*, 1752; b) S. Wingerter, M. Pfeiffer, A. Murso, C. Lustig, T. Stey, V. Chandrasekhar, D. Stalke, *J. Am. Chem. Soc.* **2001**, *123*, 1381.

[15] Review: F. Baier, Z. Fei, H. Gornitzka, A. Murso, S. Neufeld, M. Pfeiffer, I. Rüdenauer, A. Steiner, T. Stey, D. Stalke, *J. Organomet. Chem.* **2002**, *661*, 111.
[16] a) M. Albrecht, G. van Koten, *Angew. Chem.* **2001**, *113*, 3866; *Angew. Chem. Int. Ed.* **2001**, *40*, 3750; b) H. Hagen, J. Boersma, G. van Koten, *Chem. Soc. Rev.* **2002**, *31*, 357.
[17] G. Boche, *Angew. Chem.* **1989**, *101*, 286; *Angew. Chem. Int. Ed. Engl.* **1989**, *28*, 277.
[18] a) A. Müller, B. Neumüller, K. Dehnicke, *Chem. Ber.* **1996**, *129*, 253; b) A. Müller, B. Neumüller, K. Dehnicke, *Angew. Chem.* **1997**, *109*, 2447; *Angew. Chem. Int. Ed. Engl.* **1997**, *36*, 2350; c) P. B. Hitchcock, M. F. Lappert, P. G. H. Uiterweerd, Z.-X. Wang, *J. Chem. Soc. Dalton Trans.* **1999**, 3413; d) I. Fernandez, G. Alvarez, M. Julia, N. Kocher, D. Leusser, D. Stalke, J. Gonzalez, F. Lopéz-Ortiz, *J. Am. Chem. Soc.* **2002**, *124*, 15184.
[19] W.-P. Leung, Z.-X. Wang, H.-W Li, Q.-C. Yang, T. C. W. Mak, *J. Am. Chem. Soc.* **2001**, *123*, 8123.
[20] a) W. J. Knebel, R. J. Angelici, *Inorg. Chim. Acta* **1973**, *17*, 713; b) M. Alvarez, N. Lugan, R. Mathieu, *J. Chem. Soc. Dalton Trans.* **1994**, 2755.
[21] a) A. F. Cameron, N. S. Hair, D. G. Norris, *Acta Crystallogr. Sect. B* **1974**, *30*, 221; b) E. Niecke, D. Gudat, *Angew. Chem.* **1991**, *103*, 251; *Angew. Chem. Int. Ed. Engl.* **1991**, *30*, 217; c) A. Steiner, D. Stalke, *Inorg. Chem.* **1993**, *32*, 1977; d) R. Fleischer, D. Stalke, *Inorg. Chem.* **1997**, *36*, 2413.
[22] P. Rademacher, *Strukturen organischer Moleküle*, VCH, Weinheim, **1987**.
[23] a) W. N. Setzer, P. v. R. Schleyer, *Adv. Organomet. Chem.* **1985**, *24*, 353; b) C. Schade, P. v. R. Schleyer, *Adv. Organomet. Chem.* **1987**, *27*, 169; c) T. Stey, D. Stalke, Lead Structures in Lithium Organic Chemistry in *The Chemistry of Organolithium Compounds* (Eds.: Z. Rappoport, I. Marek), Wiley, Weinheim, **2003**.
[24] a) A. Steiner, D. Stalke, *J. Chem. Soc. Chem. Commun.* **1993**, 444; b) H. Gornitzka, D. Stalke, *Angew. Chem.* **1994**, *106*, 695; *Angew. Chem. Int. Ed. Engl.* **1994**, *33*, 693; c) A. Steiner, D. Stalke, *Organometallics* **1995**, *14*, 2422.
[25] R. P. K. Babu, K. Aparna, R. McDonald, R. G. Cavell, *Organometallics* **2001**, *20*, 1451.
[26] M. T. Gamer, P. W. Roesky, *Z. Anorg. Allg. Chem.* **2001**, *627*, 877.
[27] R. P. K. Babu, K. Aparna, R. McDonald, R. G. Cavell, *Inorg. Chem.* **2000**, *39*, 4981.
[28] a) K. Gregory, P. v. R. Schleyer, R. Snaith, *Adv. Inorg. Chem.* **1991**, *37*, 47; b) R. E. Mulvey, *Chem. Soc. Rev.* **1991**, *20*, 167; c) R. E. Mulvey, *Chem. Soc. Rev.* **1998**, *27*, 339.
[29] a) P. B. Hitchcock, M. F. Lappert, Z.-X. Wang, *Chem. Commun.* **1997**, 1113; b) A. Müller, B. Neumüller, K. Dehnicke, *Angew. Chem.* **1997**, *109*, 2447; *Angew. Chem. Int. Ed. Engl.* **1997**, *36*, 2350.
[30] a) T. Chivers, A. Downard, Y. P. A. Glenn, *J. Chem. Soc. Dalton Trans.* **1998**, *16*, 2603; b) T. Chivers, A. Downard, M. Parvez, *Inorg. Chem.* **1999**, *38*, 4347.
[31] A. Steiner, PhD thesis, Universität Göttingen **1994**.
[32] A. Müller, M. Möhlen, B. Neumüller, N. Faza, W. Massa, K. Dehnicke, *Z. Anorg. Allg. Chem.* **1999**, *625*, 1748.
[33] M. F. Lappert, M. J. Slade, A. Singh, J. L. Atwood, R. D. Rogers, R. Shakir, *J. Am. Chem. Soc.* **1983**, *105*, 302.
[34] A. Müller, M. Marsch, K. Harms, J. C. W. Lorenz, G. Boche, *Angew. Chem.* **1996**, *108*, 1639; *Angew. Chem. Int. Ed. Engl.* **1996**, *35*, 1518.
[35] R. I. Papasergio, B. W. Skelton, P. Twiss, A. H. White, C. L. Raston, *J. Chem. Soc. Dalton Trans.* **1990**, 1161.
[36] U. Pieper, D. Stalke, *Organometallics* **1993**, *12*, 1201.
[37] D. Hoffmann, W. Bauer, P. v. R. Schleyer, U. Pieper, D. Stalke, *Organometallics* **1993**, *12*, 1193.
[38] U. Schümann, U. Behrens, E. Weiss, *Angew. Chem.* **1989**, *101*, 481; *Angew. Chem. Int. Ed. Engl.* **1989**, *28*, 476.
[39] G. Rabe, H. W. Roesky, D. Stalke, F. Pauer, G. M. Sheldrick, *J. Organomet. Chem.* **1991**, *403*, 11.
[40] M. Veith, J. Böhnlein, V. Huch, *Chem. Ber.* **1989**, *122*, 841.
[41] a) R. Appel, *Pure Appl. Chem.* **1987**, *59*, 977; b) D. G. Gilheany in *The Chemistry of Organophosphorus Compounds, Vol. 1* (Ed.: F. R. Hartley), Wiley-Interscience, Chichester, **1990**, Chapter 2, p. 9.
[42] a) J. C. J. Bart, *J. Chem. Soc. B* **1969**, 350; b) H. Schmidbaur, A. Schlier, C. M. F. Frazao, G. Müller, *J. Am. Chem. Soc.* **1986**, *108*, 976; c) H. Schmidbaur, J. Jeong, A. Schier, W. Graf, D. L. Wilkinson, G. Müller, *New J. Chem.* **1989**, *13*, 341.
[43] a) N. K. Hansen, P. Coppens, *Acta Crystallogr. Sect. A* **1978**, *34*, 909; b) T. Koritsanszky, S. Howard, T. Richter, Z. W. Su, P. R. Mallinson, N. K. Hansen, XD—A Computer Program Package for Multipole Refinement and Analysis of Electron Densities from Diffraction Data. User Manual, Freie Universität Berlin, **1995**.
[44] R. F. W. Bader, *Atoms in Molecules—A Quantum Theory*, Clarendon Press, Oxford **1990**.
[45] Y. A. Abramov, L. Brammer, W. T. Klooster, R. M. Bullock, *Inorg. Chem.* **1998**, *37*, 6317.
[46] A. Volkov, C. Gatti, Y. A. Abramov, *Acta Crystallogr. Sect A.* **2000**, *56*, 252.
[47] W. Scherer, P. Sirsch, D. Shorokhov, G. McGrady, S. A. Mason, M. G. Gardiner, *Chem. Eur. J.* **2002**, *8*, 2324.
[48] D. Leusser, B. Walfort, D. Stalke, *Angew. Chem.* **2002**, *114*, 2183; *Angew. Chem. Int. Ed.* **2002**, *41*, 2079.
[49] a) T. Kottke, D. Stalke, *J. Appl. Crystallogr.* **1993**, *26*, 615; b) T. Kottke, R. J. Lagow, D. Stalke, *J. Appl. Crystallogr.* **1996**, *29*, 465; c) D. Stalke, *Chem. Soc. Rev.* **1998**, *27*, 171.
[50] Bruker, SMART-NT, Data Collection Software, Version 5.6, Bruker Analytical X-ray Instruments Inc., Madison, Wisconsin (USA), **2000**.
[51] Bruker, SAINT-NT, Data Reduction Software, Version 6, Bruker Analytical X-ray Instruments, Inc., Madison, Wisconsin (USA), **1999**.
[52] Bruker, SHELX-TL, Version 6, Bruker Analytical X-ray Instruments Inc., Madison, Wisconsin (USA), **2000**.
[53] G. M. Sheldrick, SADABS2, Empirical Absorption Correction Program, University of Göttingen (Germany) 2001.

Received: February 18, 2004
Published online: June 2, 2004

